Identification of candidate genomic regions for thermogelled egg yolk traits based on a genome-wide association study

Ruiqi Zhang, Xinghua Li, Ying Ma, Yuchen Liu, Yalan Zhang, Xue Cheng, and Zhonghua Ning[1]

National Engineering Laboratory for Animal Breeding, College of Animal Science and Technology, China Agricultural University, Beijing 100193, China

ABSTRACT Egg yolk texture is an important indicator for evaluating egg yolk quality. Genetic markers associated with economic traits predict genomes and facilitate mining for potential genes. Numerous genome-wide association studies have been conducted on egg traits. However, studies on the genetic basis of thermogelled yolk texture are still lacking. The aim of the present study was to find significant single nucleotide polymorphism (**SNP**) sites and candidate genes related to thermogelled yolk texture in Hetian Dahei chicken (**HTHD**) flocks that can be used as genetic markers. Five traits, including hardness, cohesiveness, gumminess, chewiness, and resilience, had low heritability (0.044−0.078). Ten genes, including *U6, FSHR, PKDCC, SLC7A11, TIMM9, ARID4A, PSMA3, ACTR10, EML4,* and *SLC35F4* may control the hardness of the thermogelled egg yolks. In addition, 12 SNPs associated with cohesiveness were identified. RELCH located on GGA2 participates in cholesterol transport. The candidate gene *LRRK2*, which is associated with gumminess, influences the concentrations of very low-density lipoprotein in blood. Eight SNPs associated with resilience were identified, mainly on GGA3 and GCA28. In total, 208 SNPs associated with chewiness were identified, and 159 candidate genes, which were mainly involved in proteasome-mediated ubiquitin-dependent protein catabolic process, negative regulation of transport, lipid droplet organization, and vehicle docking involved in exocytosis, were found near these regions. Thermogel egg yolk texture is a complex phenotype controlled by multiple genes. Based on heritability assays and GWAS results, there is a genetic basis for the texture of thermogelled egg yolks. We identified a series of SNPs associated with yolk texture and candidate genes. Our result provides a theoretical basis for breeding high-quality egg yolk using molecular marker-assisted selection and could facilitate the development of novel traits.

Key words: egg yolk texture, genetic markers, single nucleotide polymorphisms, genome-wide association study

INTRODUCTION

Consumers favor eggs because of their high nutrient contents (Zhao et al., 2021). The yolk accounts for up about 29% of the total weight of an egg (Xiao et al., 2020). Egg yolks are also a great source of high-quality protein and lipids. Dry matter in the egg yolk accounts for about 52% of the egg yolk, with fat and protein accounting for approximately 65% and 31%, respectively (Yang et al., 2020). Consumer' demand for eggs is currently fully met following an increase in egg production, and people are paying increasing attention to egg yolk quality.

Texture is an important attribute for consumers when selecting eggs. Therefore, texture quality evaluation is essential for breeding activities (Misra et al., 2018). Egg yolk texture is considered a multidimensional organoleptic property. Trained tasters can identify texture. However, they are not routinely used due to their low throughput, subjectivity, and cost implications (Sesmat and Meullenet, 2001). Texture profile analysis (**TPA**) simulates oral sensations through two compression cycles and has been used extensively to study the textures of various materials. It provides information about the mechanics, including hardness (**HAR**), springiness (**SPR**), cohesiveness (**COH**), gumminess (**GUM**), chewiness (**CHE**), and resilience (**RES**) of a material.

During heating processes, deformed protein molecules in the egg aggregate and undergo orderly folding, forming a gel. Gel formation improves the texture of the yolk, and the egg yolk components could influence the texture. For example, protein content influences the texture of the thermogelled egg yolks (**TEY**) (Debusca et al., 2013),

and previous studies have reported that increased lipid content in egg yolks reduces the cohesiveness of TEY and improves egg yolk texture (Zhang et al., 2022).

Yolk texture is a key factor considered by egg consumers, and many consumers do not like the texture of TEY (Perea et al., 2016). Therefore, improving the texture of egg yolks through breeding approaches would increase consumer preference for certain egg yolks (Winham et al., 2019). Pena et al. showed that 7 QTLs influence pork texture, and genetic factors in pigs can affect the perception of sensory attributes of processed dry-cured ham (Pena et al., 2013). Genetic studies on texture have been carried out extensively in plants; however, no studies have been carried out on TEY texture.

Recently, genome-wide association studies (**GWAS**) have been used widely in animal and plant breeding studies. GWAS can combine phenotypes and genotypes to dissect the genetic basis of various complex phenotypes (Xiao et al., 2017). Furthermore, it identifies candidate genes associated with target traits through a series of sequencing, alignment, and analysis activities (Wen et al., 2018). To the best of our knowledge, no GWAS analysis has been performed to identify potential candidate genes that influence TEY texture.

The aim of the present study was to identify significant SNP sites and candidate genes related to TEY texture in Hetian Dahei chicken (**HTDH**) flocks, which can be used as genetic markers, based on TPA results, sequencing methods, and GWAS. The results of the present study could enhance our understanding of the genetic bases and underlying mechanisms of TEY texture.

MATERIALS AND METHODS

All experimental procedures were performed in accordance with the National Institutes of Health Guide for the Care and Use of Laboratory Animals (NIH Publications No. 8023, revised in 1978) and all experiments on chicken embryos were performed in accordance with the protocol outlined in the "Guide for Care and Use of Laboratory Animals" (China Agricultural University).

Animals and Sample Collection

RIR and HTDH hens were collected from Hebei Rongde Breeding Company, and eggs laid within 24 h were randomly selected during sampling. In total, 430 HTDH eggs and 412 RIR eggs were used in the previous study. This study used 200 HTDH blood samples from Hebei province, China. A blood sample of each female chick for GWAS was collected from the wing vein using 1 mL injectors at 42 wk of age. All the egg-laying hens were raised in separate cages under identical conditions and fed the same feed throughout the experiment.

Texture Profile Analysis of Boiled-egg Yolks

All eggs were pretreated as follows. One minute after boiling water, the eggs were added and boiled for 5 min,

and the heat was turned off. After 3 min, the eggs were removed from the hot water, and the entire yolk was separated from the egg albumin by hand and prepared for analysis at room temperature (26°C). A TA-XT2i texture profile analyzer (TPA; Texture Technologies, Scarsdale, NY) with a P50 probe was used to evaluate the texture characteristics of the cooked egg yolks.

Heritability

Variance and covariance components were estimated using the DMU software package (swMATH, Berlin, Germany). The heritabilities of HAR, SPR, COH, GUM, CHE, and RES were analyzed using an animal threshold model based on the following equation:

$$y = X\beta + Za + e$$

where y = vector of phenotypic values; β = vector of fixed effects, a = vector of random additive genetic effects for all individuals, e = vector of random residuals, and X and Z are appropriate association matrices. Animal thresholds were analyzed using the Gibbs sampling module included in the DMU software package (Ødegård et al., 2010), and classic animal models were analyzed using the Mean Information Restricted Maximum Likelihood (AI-REML) algorithm using the DMUAI module in DMU (Li et al., 2018).

Genotyping and Quality Control

We isolated individual genomic DNA from blood samples using the phenol-chloroform method. Purity was analyzed using a NanoDrop 2000 spectrophotometer (Thermo Fisher Scientific Inc., Waltham, MA). Whole-genome sequencing was performed using the T7 platform (Beijing Genomics Institute, Shenzhen, China). Plink v1.9 was used for quality control (Purcell et al., 2007). During quality control, SNPs with an allele frequency of $\geq 1\%$ and a genotyping rate of $\geq 98\%$ were retained. Individuals with a genotype deletion rate of >5% were eliminated. SNPs with $P < 10^{-6}$ using the Hardy-Weinberg Equilibrium were eliminated. After filtering, 194 chickens were retained for further analysis.

Population Structure Analysis

Before GWAS, we assessed the population structure using Principal Component Analysis (**PCA**) using the PLINK software package (William and David, 2009). PLINK 1.9 was used to determine the overall structure and generate eigenvectors and eigenvalues; relatively dependent SNPs were preserved using the plink '−indep-pairwise 25 5 0.2′ command. The results of PCA were visualized as a plot using the first two principal components as horizontal and vertical coordinates, using the "ggplot2" package in R studio (R Foundation for Statistical Computing, Vienna, Austria).

Genome-Wide Association Studies

The five texture traits were subjected to GWAS using univariate linear mixed models in GEMMA (Zhou and Stephens, 2012). The model is based on the following equation:

$$y = W\alpha + x\beta + u + \varepsilon$$

where y represents an n × 1-dimensional quantitative trait phenotype value vector of phenotype values, W is a covariate matrix, α represents a vector of corresponding coefficients consisting of intercepts, x is a vector of marker genotypes, β is the corresponding effect of the SNP, u is a vector of random polygenic effects whose covariance structure obeys a normal distribution, u~N (0, KVg), where K is the genomic relationship matrix derived from independent SNPs, Vg is the polygenic additive variance, and ε is the error vector. In the present study, the Wald test (Shen et al., 2016) was used as a criterion for selecting SNPs associated with the metabolizable efficiency trait.

Manhattan and quantile-quantile (**Q-Q**) plots were drawn using the "qqman" package in R (R Foundation for Statistical Computing). The traditional Bonferroni correction was too strict, resulting in a high false-negative rate and missing of some SNPs that are truly associated with the target trait (Bland and Altman, 1995). Therefore, independent tests were performed using simpleA, setting the genome-wide significance and prompt thresholds to 3.71×10^{-8} (0.05/1, 346, 502) and 7.43×10^{-7} (1/1, 346, 502), respectively.

Bioinformatics Analysis of Candidate Genes

We searched for the nearest genes 100 kb upstream or downstream of the significantly related SNPs to identify candidate genes annotated according to Galgal 6.0 assemblies supported by Biomart tools in the Ensembl (http://www.ensembl.org/index.html) database. We then searched PubMed (https://pubmed.ncbi.nlm.nih.gov) for the biological functions of the genes.

Overlapping with Known QTL

The chicken QTL database was searched for QTLs related to fat, protein, and texture within 100 kb of candidate SNPs (https://www.animalgenome.org/cgi-bin/QTLdb/GG/index).

RESULTS

Heritability

The texture of TEY from the animals has been reported previously (Zhang et al., 2022). The texture of TEY is evaluated mainly based on 6 indicators, namely HAR, SPR, COH, GUM, CHE, and RES; all 6 indicators exhibit a continuous normal distribution. There were significant differences in egg yolk texture between and within varieties.

The results of the heritability test are presented in Table 1. CHE had the highest heritability (0.078), while SPR had the lowest heritability (0). HAR, COH, GUM, CHE, and RES had low heritability (0.044−0.078). The low heritability of HAR, COH, GUM, CHE, and RES in the texture analyzer indicates the genetic basis of egg yolk texture.

Population Structure Tests

The texture of TEY was measured using a texture analyzer. The TPA results included HAR, SPR, COH, GUM, CHE, and RES; these results have been previously reported (Zhang et al., 2022). Because SPR heritability was 0, no GWAS was performed for SPR.

A total of 200 samples were sequenced, and after a series of stringent quality control procedures, 6 samples were eliminated due to poor sequencing quality. Consequently, the final GWAS population consisted of 194 samples. In GWAS, population stratification can lead to false-positive results. However, PCA based on the first two principal components showed that the experimental population was not stratified (Figure 1). The Genomic Inflation Factor (λ) was simultaneously calculated. The λ values of HAR, COH, GUM, CHE, and RES were 1.053, 1.057, 1.047, 1.069, and 0.927, respectively. These values were close to 1; therefore, they could be applied in GWAS.

Genome-Wide Association Studies

GWAS were performed using HAR, COH, GUM, CHE, and RES as quantitative traits. We use the value of 0.05/SNP number to determine the significance and potential threshold of the whole genome, setting the genome-wide significance and prompt thresholds to 3.71×10^{-8} (0.05/1, 346, 502) and 7.43×10^{-7} (1/1, 346, 502), respectively.

The Manhattan and Q-Q plots of HAR are shown in Figure 2a, b. The Q-Q plot (Figure 2a) indicated no delamination and that the GWAS results were reliable. The Manhattan plot shows a global view of P-values (expressed as $-\log10[P$-values]) for all SNPs (Figure 2b). We found 8 SNPs significantly associated and 98 potentially associated with HAR (Table S1). The SNPs associated with HAR were mainly located on chromosomes 1, 3, 4, and 5. Associated SNPs were annotated in Ensembl using a 100 K-b (kilobase) window near the locus (Table 2). We found 10 genes around the significant sites, namely *U6, FSHR, EML4, PKDCC,*

Table 1. Heritabilities of the texture profile analysis.

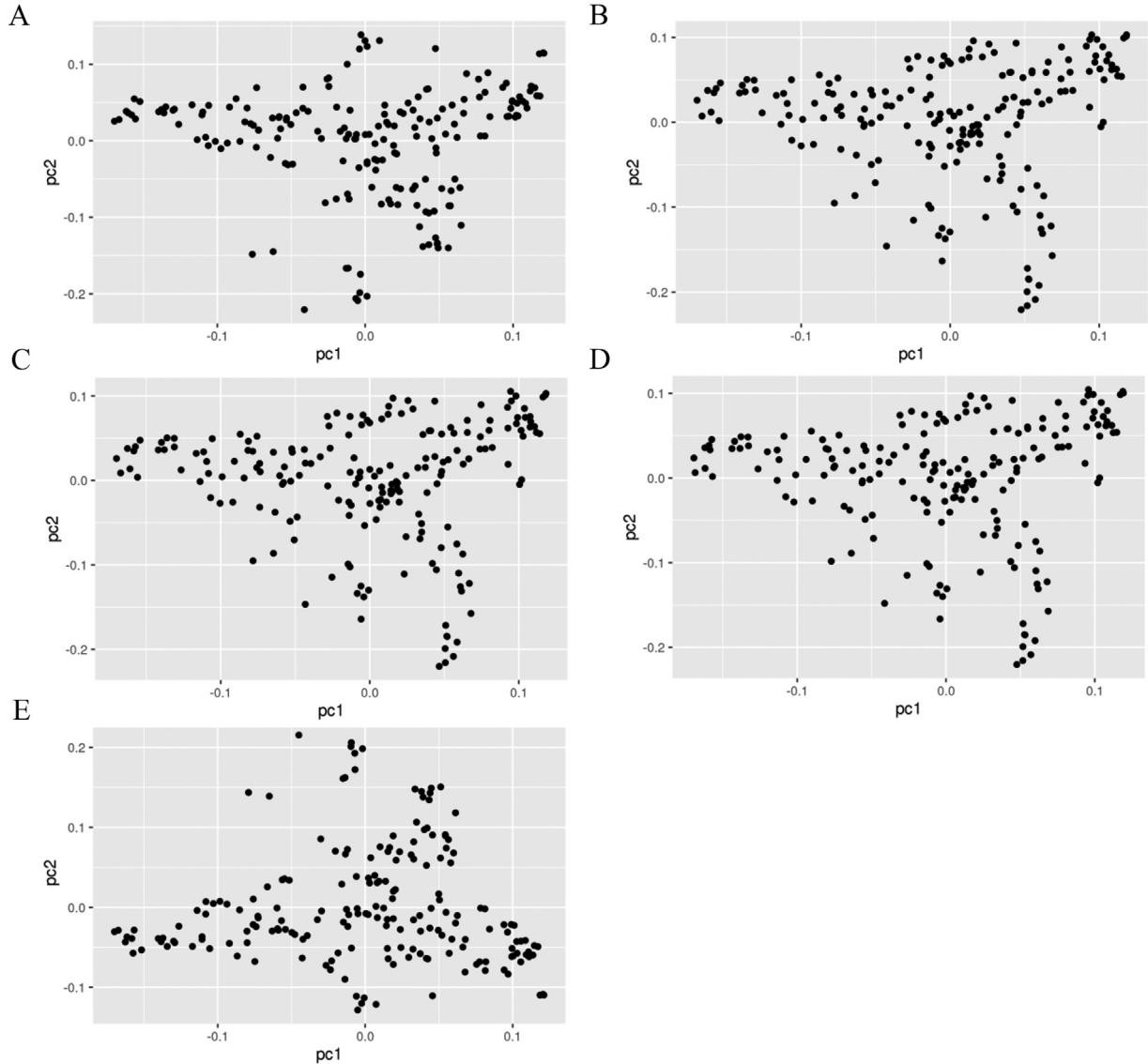| Species	Heritability	SE
Hardness	0.054	0.059
Springiness	0.00	0.061
Cohesiveness	0.053	0.065
Gumminess	0.044	0.062
Chewiness	0.077	0.067
Resilience	0.055	0.066

Figure 1. Principal Components Analysis (PCA) plot of the flocks in this study. The abscissa is the first principal component, and the ordinate is the second principal component. a: hardness (HAR); b: cohesiveness (COH); c: gumminess (GUM); d: chewiness (CHE); e: resilience (RES).

SLC7A11, TIMM9, ARID4A, PSMA3, ACTR10, and *SLC35F4.*The most important peaks were located at 7.05 to 8.29 Mb and 22.67 to 23.96 Mb on GGA3 and 28.02 to 28.92 Mb on GGA4. We repeatedly identified 5 genes in the regions: *FSHR, U6, SLC35F4, SLC7A11, PKDCC.*

The Manhattan and Q-Q plots of COH are shown in Figure 2c, d. The Q-Q plot (Figure 2c) indicates no stratification phenomenon, and the GWAS results were reliable. Manhattan plots show a global view of *P*-values (expressed as −log10 [*P*-values]) for all SNPs (Figure 2d). We found 12 SNPs potentially associated with COH (Table S1). Because there were no significant sites, we annotated potential sites. The SNPs associated with COH were mainly located on chromosomes 2, 6, 14, and 21. Associated SNPs were annotated using Ensembl and a 100-Kb window near the locus (Table 2). The most important peak was located at 68.41 to 80.49 Mb on GGA2. We identified eight genes involved in SNPs: *PIGN, RNF152,* FIGNL1, RELCH, *EPN2,* ARMH3, DDC, *NPM3.*

Figure 2e, f shows the Manhattan and Q-Q graphs of GUM. The Manhattan plot shows *P*-values (expressed as −log10[*P*-values]) for all SNPs. we found 336 SNPs (37 significant sites, 299 potential sites) associated with GUM. The significant SNPs were mainly concentrated on chromosomes 1, 2, 5, 15, and 21. We annotated 100-Kb regions near SNPs with Ensembl to find candidate genes. Significant SNPs were mainly concentrated in GGA1 at 15.15 to 24.99 Mb.

The Manhattan and Q-Q plots of the CHE are shown in Figure 3a, b. The Q-Q plot (Figure 3a) indicates that mild delamination occurs; however, this does not affect the GWAS results. The Manhattan plot presents a global view of *P*-values (expressed as −log10[*P*-values]) for all SNPs (Figure 3b). We found 754 SNPs (208 significant loci, 546 potential loci) that may be associated with CHE (Table S1). The SNPs associated with CHE were mainly located on GGA1, 3, 4, and 13. Associated SNPs were annotated using Ensembl and a 100-Kb window near the locus (Table 2). We performed Gene
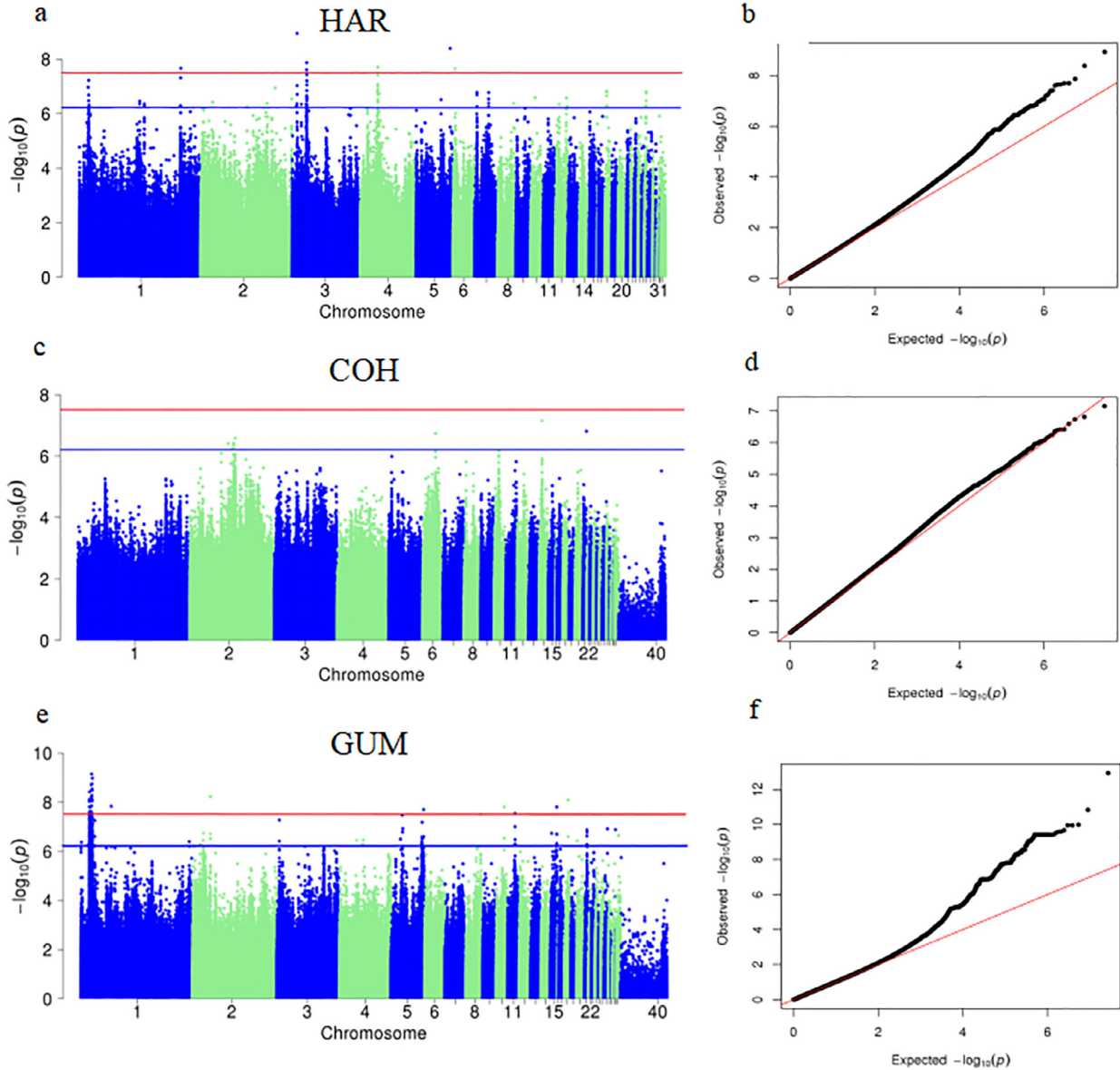
Figure 2. Q-Q plot and Texture Profile Analysis (TPA) traits in Manhattan Plot. The Q-Q plot shows the expected −log10 P-value (x-axis) vs. the observed −log10 P-value (y-axis). In the Manhattan plot, the x-axis is the position of each SNP on the chicken chromosome (40 means Z chromosome), and the y-axis is the −log10 P-value. The horizontal red dashed line at the top represents the genome-wide significance threshold of 3.71×10^{-8}, and the bottom line represents the genome-wide implication threshold of 7.43×10^{-7}. a: Manhattan plot of hardness (HAR); b: Q-Q of HAR.

Ontology (GO) analysis on candidate genes near the SNPs of significant loci (Figure 4). The main enriched GO terms were proteasome-mediated ubiquitin-dependent protein catabolic process, negative regulation of transport, lipid droplet organization, and vesicle docking involved in exocytosis.

Figure 3c and d show the Manhattan and Q-Q plots of RES. The Manhattan plot shows P-values for all SNPs. We found 8 SNPs (4 significant sites, 4 potential sites) that may be associated with RES. The significant SNPs of RES were mainly concentrated on GGA3 and 28. A 100-Kb window near the SNPs was annotated with Ensembl to find candidate genes. Significant SNPs were mainly concentrated on GGA3 at 56.49 to 56.78 Mb.

Comparison to Previously Reported QTL

By comparing the results from this study with previously reported QTLs, we detected 9 overlapping QTLs; 5 were associated with body fat, and one had effects on very-low-density lipoprotein and cholesterol.

DISCUSSION

The texture of TEY is a key factor influencing consumer acceptance and preference for egg yolks. Although numerous studies have been conducted on the textural properties of TEY (Sun et al., 2021; Zhang et al., 2022), the genetic factors underlying the textures remain unclear. Previous research has reported that TEY

Table 2. Genome-wide SNPs around significant peaks associated with TEY traits.

Type	Chr	SNP	P value	Nearest gene
HAR	1	165613340	2.21E−08	
	3	8023505	1.16E−09	U6,FSHR
	3	23726670	1.36E−08	EML4
	3	23545065	2.49E−08	PKDCC
	4	28831930	1.99E−08	SLC7A11
	4	28845715	1.99E−08	SLC7A11
	5	55503318	4.11E−09	TIMM9,ARID4A,PSMA3, ACTR10,SLC35F4
	6	4268540	2.26E−08	TIMM9,ARID4A,PSMA3, ACTR10,SLC35F4
COH	2	68411379	3.86E−07	RELCH,PIGN,gga-mir-1782, RNF152
	2	74549300	5.95E−07	
	2	77642989	4.40E−07	
	2	77652835	4.05E−07	
	2	77823176	5.77E−07	gga-mir-1613
	2	77838234	3.80E−07	gga-mir-1613
	2	80699665	2.60E−07	SPATA48,IKZF1,FIGNL1, DDC
	6	23621670	1.84E−07	ARMH3,KCNIP2,MGEA5, NPM3,FGF8,POLL
	6	23683402	7.21E−07	ARMH3,KCNIP2,MGEA5, NPM3,FGF8,POLL,DPCD, gga-mir-1674
	10	9154088	6.63E−07	ONECUT1,FAM214A, ARPP19,MYO5A
	14	5545951	7.11E−08	ALKBH5,LLGL1,FLII,MIEF2, TOP3A,SMCR8,SHMT1, PRPSAP2,SLC5A10, FAM83G,GRAPL,EPN2, gga-mir-1551,B9D1
	21	6779571	1.56E−07	EIF4G3,HP1BP3,SH2D5, DDOST
GUM	1	20537868	1.04429E−09	SELENOO,TUBGCP6, HDAC10,MAPK12,MAPK11
	1	15150402	7.66702E−09	LAMB1, LAMB4, ERGIC2, LRRK2, SLC2A13
	1	15194616	9.35362E−09	LAMB1, LAMB4, ERGIC2, LRRK2, SLC2A13
	1	19157061	1.40311E−08	
	1	54048433	1.45042E−08	NUAK1
	1	15217019	1.53838E−08	LAMB1, LAMB4, ERGIC2, LRRK2, SLC2A13
	1	17329884	1.54619E−08	TAFA5
	1	18322461	2.3947E−08	
	1	16552021	2.41901E−08	TBC1D22A
	1	15190569	2.51495E−08	LAMB1, LAMB4, ERGIC2, LRRK2, SLC2A13
	1	17465325	2.6095E−08	TAFA5
	1	17329769	2.83011E−08	TAFA5
	1	20308589	2.9408E−08	IL17REL, MLC1, MOV10L1, PANX2, TRABD
	1	15470197	3.01236E−08	SLC2A13, ABCD2, KIF21A
	1	16484836	3.06594E−08	TBC1D22A
CHE	1	88874780	4.00811E−09	MYH15,KIAA1524,SH2D1B, TRAT1,HJURP,GUCA1C
	1	88875570	4.00811E−09	MYH15,KIAA1524,SH2D1B, TRAT1,HJURP,GUCA1C
	1	84752783	4.00857E−09	CCDC80,SLC35A5,ATG3,F5, SLC19A2,CCDC181,BLZF1, NME7
	1	84753795	4.00857E−09	CCDC80,SLC35A5,ATG3,F5, SLC19A2,CCDC181,BLZF1, NME7
	1	86457528	2.18533E−08	IMPG2,SENP7,TXNL4B, TRMT10C,PCNP,ZBTB11, RPL24,NXPE3,NFKBIZ
	1	130355385	2.33144E−08	ASMT,AKAP17A,P2RY8, ASMTL,SLC25A6
	2	130955385	1.90579E−08	BOP1,SCX,HSF1
	2	23245547	2.28941E−08	CALCR,TFPI2
	3	8557985	1.15378E−13	CAPN13,LCLAT1
	3	8411640	1.44997E−11	

(continued)

Table 2 (*Continued*)

Type	Chr	SNP	P value	Nearest gene
				EHD3,CAPN14,GALNT14, gga-mir-1792,CAPN13
	3	71454823	9.62985E−09	PRDM13,CCNC,USP45, PNISR,COQ3,FAXC
	3	13762174	1.5274E−08	SLX4IP,MKKS,SNAP25
	3	7606680	1.85481E−08	NRXN1
	3	70648983	1.85481E−08	ASCC3
	3	19136791	2.03887E−08	LYPLAL1
	3	20177434	4.66957E−08	ESRRG
	3	71455175	2.13096E−08	PRDM13,CCNC,USP45, PNISR,COQ3,FAXC
	4	89993843	5.38278E−09	EXOC6B,gga-mir-12276
	4	4855617	1.36652E−08	FGF13
	4	90887270	1.50659E−08	LOXL3,HTRA2,AUP1,DQX1, PCGF1,LBX2,TTC31, MOGS,WBP1,RTKN, WDR54
	10	18042010	6.47179E−09	LRRK1,CHSY1,SELENOS, SNRPA1,PCSK6
	13	16521197	5.30056E−10	SEC24A,SAR1B,JADE2, UBE2B,PPP2CA,SKP1, TCF7
	13	16521285	5.46082E−10	SEC24A,SAR1B,JADE2, UBE2B,PPP2CA,SKP1, TCF7
	13	16708074	6.53857E−09	PPP2CA,SKP1,TCF7,VDAC1, C13H5orf15
	20	9879296	2.88177E−08	STK35,SIRPA,gga-mir-12243, NSFL1C,FKBP1A,SDCBP2, SNPH,RAD21L1,PSMF1, RSPO4,ANGPT4,SLC52A3, SCRT2,SRXN1,TCF15, CSNK2A1,TBC1D20
	20	9879302	2.88177E−08	STK35,SIRPA,gga-mir-12243, NSFL1C,FKBP1A,SDCBP2, SNPH,RAD21L1,PSMF1, RSPO4,ANGPT4,SLC52A3, SCRT2,SRXN1,TCF15, CSNK2A1,TBC1D20
	22	2530600	1.50659E−08	ZNF703,ERLIN2,PLPBP, ADGRA2,BRF2,RAB11- FIP1,PRLHRL,EIF4EBP1, ASH2L,STAR,LSM1,BAG4, DDHD2,PLPP5,NSD3
RES	3	5671381	2.45E−08	SNRPB2,CTAGE1
	3	5675746	2.45E−08	SNRPB2,CTAGE1
	3	5678091	2.58E−08	SNRPB2,CTAGE1
	28	2892042	1.15E−08	HCN2,POLRMT,FGF22, RNF126,FSTL3,PALM, PTBP1,PLPPR3,CFD, MED16,U6,R3HDM4, ARID3A,WDR18,GRIN3B, TMEM259

texture is associated with the lipids and proteins contained in the egg yolk. Yolk texture becomes more delicate as the lipid concentrations in yolk increase (Zhang et al., 2022). The aim of the present study was to identify potential candidate genes associated with genetic variation in 5 texture indicators using blood samples from 200 HTDH hens.

In studies on heritability in chickens, more traits have low heritability. For example, the antimicrobial heritability in the chicken cecum is 0.06 (Berthelot et al., 1998), and heritability estimates for hatchability of eggs from laying hens are 0.007 to 0.08 (Rozempolska-Rucinska et al., 2013). This study is the first to determine heritability estimates for TEY texture. The
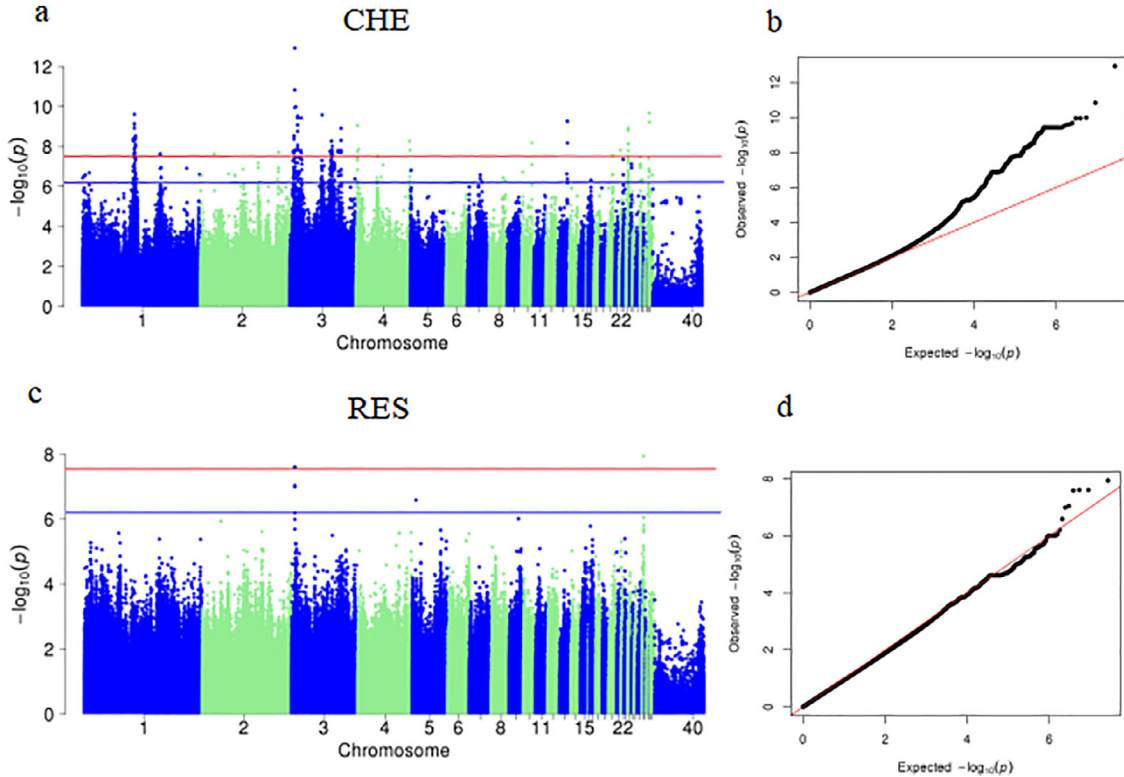
Figure 3. Q-Q plot and cohesiveness traits in Manhattan. The Q-Q plot shows the expected $-\log10$ P-value (x-axis) vs. the observed $-\log10$ P-value (y-axis). In the Manhattan plot, the x-axis is the position of each Single Nucleotide Polymorphism (SNP) on the chicken chromosome (40 means Z chromosome), and the y-axis is the $-\log10$ P-value. The horizontal red dashed line at the top represents the genome-wide significance threshold of 3.71×10^{-8}, and the bottom line represents the genome-wide implication threshold of 7.43×10^{-7}. a: Manhattan plot of chewiness (CHE); b: Q-Q plot of CHE; c: Manhattan plot of resilience (RES); d: Q-Q plot of RES.

low heritability in HTDH may be due to lack of selection for the trait in the breed. TEY texture is influenced by numerous factors, including breed, feed, and environment. The HAR, COH, GUM, CHE, and RES of egg yolks were significantly reduced after storage at 25°C compared to eggs stored at 4°C (Zhu et al., 2019). HAR, COH, GUM, CHE, and RES showed low heritability using the texture analyzer, indicating the genetic basis of TEY texture. Heritability estimates for the same trait in different breeds can be biased, and the low heritability of HTDH may be due to lack of

selection for the trait in the breed. Heritability estimates are the basis for poultry breeding for TEY texture.

After determining texture phenotype and heritability, we investigated the genetic basis of texture in 200 HTDH chickens by performing GWAS using blood samples. This is the first study on the texture of TEY from a genetic basis. For HAR, we identified 10 candidate genes. Egg yolks develop from hen follicles. *FSHR* is selectively expressed in ovarian granulosa cells, and its expression level is closely related to germ cell
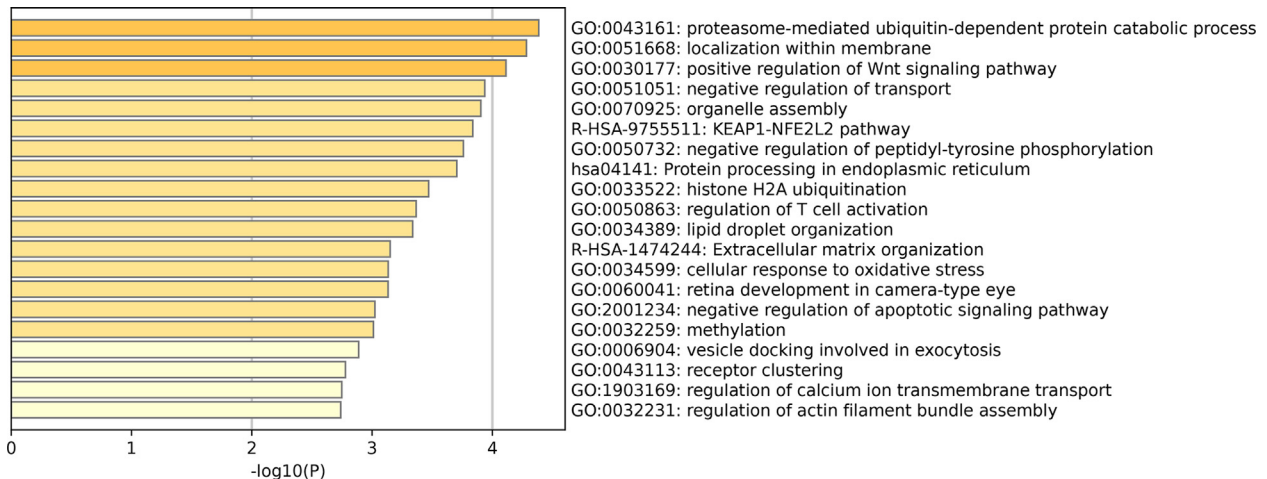

Figure 4. Heatmap of the top 20 candidate gene clusters and their representative enriched terms for chewiness (CHE).

differentiation and maturation (Li et al., 2019). The *U6* promoter is the most commonly used type of promoter in vector shRNA expression systems (Bannister et al., 2007). *SLC35F4* is a member of the solute vector family 35 F4, which can affect dairy products by regulating fatty acids in milk in dairy cows (Goyache et al., 2021). Cystine uptake is closely related to the expression of *SLC7A11*, a component of System X c-sodium-dependent amino acid counterparts (Choi et al., 2020). The function of the *PKDCC* gene has not been annotated; therefore, its function in chickens is unknown.

FSHR plays an essential role in ovarian development (Li et al., 2019). FSHR is a member of the G protein-coupled receptor glycoprotein family and interacts with FSH to regulate fat synthesis. FSH stimulates lipid biosynthesis and improves chicken meat quality by upregulating FSHR mRNA expression in chicken abdominal adipose tissue (Sun et al., 2013). FSHR improves the HAR of TEY by stimulating lipid synthesis in the ovary. PKDCC is a protein kinase containing a cytoplasmic protein kinase domain and the GO entry is protein phosphorylation. Therefore, it could affect the entry of phosphate groups into proteins and as well as the transport of proteins (Vitorino et al., 2015). In addition, by affecting the structure and transport of proteins, it influences the HAR of TEY. Therefore, it is reasonable to speculate that FSHR and PKDCC influence the HAR of TEY.

For COH, we found 28 candidate genes near the SNP. RELCH is a Rab11-GTP-binding protein involved in the transport and distribution of cholesterol through interaction with *OSBP* (Sobajima et al., 2018). *PIGN* encodes an enzyme involved in the biosynthesis of glycosylphosphatidylinositol, which anchors various proteins to the cell surface (Tian et al., 2022). *RNF152* regulates body fat production (Silva et al., 2019). In addition, FIGNL1 is a protein involved in the repair of DNA double-strand breaks through homologous recombination in mitotic cells (Govindaraj and Rao, 2015). *EPN2* is involved in protein and lipid endocytosis (Lu and Drubin, 2017). ARMH3 is a binding partner of PI4KA and participates in the production of the lipid phosphatidylinositol (Mcphail and Burke, 2022). DDC is an enzyme directly involved in synthesizing dopamine and serotonin (Zhang et al., 2004). *NPM3* is a member of the nucleophospholipid/nucleoplasmin family and encodes a protein associated with nuclear chaperone phosphorylation, plasmin, and nucleophospholipid (Macarthur and Shackleford, 1997).

Five candidate genes were identified based on their functions. RELCH plays an essential role in the transport of cholesterol and harbor numerous phosphorylation sites that facilitate the entry of cholesterol into cells. Increased cholesterol in the ovaries reduces the COH of thermogelled egg yolks (Sobajima et al., 2018). The mTOR pathway is involved in cellular metabolism, survival, and proliferation by regulating anabolic processes, including protein, lipid, and nucleotide synthesis. *RNF152*, located on GGA2, regulates the mTOR pathway and participates in the production of lipids in egg yolk (Zhang et al., 2021). *FIGNL1* is located on GGA2

and is expressed in mouse follicles. FIGNL1 is a member of a subfamily of ATPases associated with multiple cell-active protein families that regulate adenosine triphosphate hydrolysis activity (Govindaraj and Rao, 2015). DDC located on GGA2 is also an aromatic L-amino acid decarboxylase, as it has been demonstrated to decarboxylate other aromatic L-amino acids such as tryptophan, histidine, and phenylalanine (Papatsirou et al., 2021). It can catalyze the non-hydrolytic addition to or removal of carboxyl groups from compounds. It can also catalyze the cleavage of C-C bonds or add groups to double bonds (Guenter and Lenartowski, 2016). DDC can change the protein structure in egg yolk and improve the cohesiveness of egg yolk. PI4KB can regulate the production and transport of lipids. ARMH3 is located on GGA6 and has been identified as the binding partner of PI4KB. Some studies have found that the knockdown of ARMH3 can reduce PI4KB levels (Mcphail and Burke, 2022). ARMH3 affects PI4KB and increases phosphatidylinositol in egg yolk, reducing cohesiveness.

Candidate genes that may affect GUM are *LAMB1, ERGIC2, LRRK2, ABCD2, TBC1D22A, PIM3,* and *MAPK12*. These candidate genes primarily affect protein, lipid, and transmembrane transport. *LAMB1* participates in follicle development and indirectly affects the secretion of estradiol in follicles (Kulus et al., 2021). Phosphorylation sites in LAMB1 play a regulatory role over protein function, LAMB1 promotes protein phosphorylation and influence protein structure, and protein tertiary structure in turn affects the spatial structure of TEY and improves GUM (Kulus et al., 2021). The ERGIC2 protein is an endoplasmic reticulum resident protein (Yu et al., 2014). The ERGIC2 protein is an endoplasmic reticulum resident protein involved in protein trafficking between the endoplasmic reticulum and the Golgi intermediate region, the cis-Golgi (Yu et al., 2014). *LRRK2* affects the concentrations of very-low-density lipoprotein in blood (Zhang et al., 2019). ABCD2 is a peroxisomal transporter that is abundant in adipose tissue and promotes the oxidation of long-chain monounsaturated fatty acids (Liu et al., 2012). LRRK2 and ABCD2 located on GGA1 are important genes of blood very-low-density lipoprotein (Zhang et al., 2019), and very-low-density lipoprotein is an essential substance required for the formation of triglycerides and low-density lipoprotein. LRRK2 and ABCD2 promote lipid production in the body. Compared with wild mice, LRRK2 knockout mice have higher serum cholesterol (Baptista et al., 2013). SLC2A13 is a plasma membrane inositol transporter involved in the transport of inositol and glucose (Pillai et al., 2021). PIM3 regulates downstream protein activity through phosphorylation (Wang et al., 2019), and MAPK12 is involved in protein phosphorylation (Najar et al., 2022). TBC1D22A interacts with the Rab family responsible for membrane trafficking and intracellular signaling and participates in transmembrane transport (Liu et al., 2018). TBC1D22A transports lipids to the egg yolk and increases the GUM of the egg yolk (Liu et al., 2018).

In the CHE analyses, some genes were involved in the proteasome-mediated ubiquitin-dependent protein catabolic process, including *AUP1, SKP1, UBE2B, PSMF1, ASCC3, ERLIN2, SELENOS, NSFL1C, PCNP, HTRA2, USP45, LYPLAL1. AUP1, DDHD2, TBC1D20,* and *ESRRG* participate in lipid droplet organization. *SNAP25, BLZF1, EXOC6B,* and *EHD3* participate in vehicle docking during exocytosis. In addition, *AUP1*, which is located on GGA4, participates in lipid metabolism and has a positive effect on intramuscular fat deposition, and AUP1, a CUE domain protein, participates in lipid droplet formation and induces lipid droplet aggregation, increasing lipid deposition in TEY and improving TEY quality (Weng et al., 2022). *UBE2B* is located on GGA13 and participates in lipid metabolism. *UBE2B* is consistent with the QTL of beef meat quality traits. *UBE2B* can participate in ubiquitin-mediated protein degradation, affecting lipids and proteins in TEY. Therefore, it is reasonable to speculate that it is involved in the CHE of TEY (Dai et al., 2018). Lipids and proteins are transported through the blood and enter the yolk by endocytosis. *EHD3* located on GGA3 is involved in endocytosis and regulates the entry of lipids and proteins into the yolk, and changes in lipid and protein content in the yolk affect its texture (Galperin et al., 2002). Studies have demonstrated that *ESRRG* can directly control the expression of specific genes involved in lipid and lipoprotein metabolism and mitochondrial function (Sanoudou et al., 2010). Estrogen-related receptor gamma, which is encoded by *ESRRG*, is an orphan nuclear receptor that regulates triglycerides and lipid metabolism. *ESRRG* is involved in the production of LIPIN1 and facilitates the production of hepatic diacylglycerol, which is the direct precursor of triglycerides. *ESRRG* is involved in the production of triglycerides in the serum and regulates hepatic very-low-density lipoprotein- triglycerides secretion (Chen et al., 2019).

Several genes affect egg yolk resilience. *FGF22* selectively promotes excitatory presynaptic differentiation and participated in follicular development and luteal differentiation (Castilho et al., 2019). *RNF126* plays a role in different physiological processes dependent or independent of E3 ligase activity (Xu et al., 2021). FSTL3 is involved in dyslipidemia and inflammation as an adipokine and is essential for normal folliculogenesis and embryonic development, whereas *FSTL3* promotes lipid accumulation in macrophages (Runhua et al., 2019). PTBP1 (polypyrimidine tract binding protein 1) is an RNA-binding protein, a specific inhibitor of mRNA splicing in the mammalian nervous system (Medina et al., 2011). *CFD* promotes adipocyte differentiation and promotes adipogenesis (Song et al., 2016), and *GRIN3B* affects beef quality (Hofmann et al., 2022).

As a novel cytokine, FSTL3 located on GGA28 regulates lipid homeostasis and increases lipid accumulation (Sun et al., 2019). In addition, it participates in follicle development and formation (Runhua et al., 2019). PTBP1 is a splicing regulatory protein with multiple functions, acting as a post-transcriptional regulator of many processes. It regulates cholesterol biosynthesis by regulating 3-hydroxy-3-methylglutaryl-CoA reductase and the low-density lipoprotein receptor, which are involved in cholesterol biosynthesis (Medina et al., 2011). In addition, FGF22, located on GGA28, is a fibroblast growth factor that regulates follicular and luteal development (Castilho et al., 2019), whereas RNF126 is a ring domain-containing protein involved in proteasome-mediated ubiquitin-dependent protein catabolism (Xu et al., 2021).

Nine SNP effects observed in the present study are consistent with the QTLs of previous studies. Among the overlapping QTLs, five were fat-related, with one being very-low-density lipoprotein related, supporting the results of this study.

However, some of the genes identified in the present study, such as *PKDCC, RNF152, ERGIC2,* and *FSTL3*, have never been studied in chickens before. The results of this study could pave the way for future research on the relationship between the genes and egg yolk texture. In addition, the specific functions of the genes require further validation.

In the present study, GWAS was performed based on differences in the texture of TEY of different varieties. A series of SNPs and candidate genes related to TEY texture were identified based on 5 texture indicators (i.e., HAR, COH, GUM, CHE, and RES), and nine SNPs overlapped with previously reported QTL regions. The results enhance our understanding of the genetic basis for egg yolk texture and facilitate the leveraging of phenotypic and genotypic data for an enhanced understanding of genetic structure.

ACKNOWLEDGMENTS

DISCLOSURES

No conflict of interest exists in the submission of this manuscript, and manuscript is approved by all authors for publication. On behalf of all the authors, I declare that this paper is original and none of the material in the paper has been published or is under consideration for publication elsewhere. All the authors listed have read the manuscript and approved the submission of the paper to your journal.

SUPPLEMENTARY MATERIALS

Supplementary material associated with this article can be found in the online version at doi:10.1016/j.psj.2022.102402.

REFERENCES

Bannister, S. C., T. G. Wise, D. M. Cahill, and T. J. Doran. 2007. Comparison of chicken 7SK and U6 RNA polymerase III promoters for short hairpin RNA expression. BMC Biotechnol. 7:79.

Baptista, M. A., K. D. Dave, M. A. Frasier, T. B. Sherer, M. Greeley, M. J. Beck, J. S. Varsho, G. A. Parker, C. Moore, M. J. Churchill, C. K. Meshul, and B. K. Fiske. 2013. Loss of leucine-rich repeat kinase 2 (LRRK2) in rats leads to progressive abnormal phenotypes in peripheral organs. PLoS One 8:e80705.

Berthelot, F., C. Beaumont, F. Mompart, O. Girard-Santosuosso, P. Pardon, and M. Duchet-Suchaux. 1998. Estimated heritability of the resistance to cecal carrier state of Salmonella enteritidis in chickens. Poultr. Sci. 77:797–801.

Bland, J. M., and D. G. Altman. 1995. Multiple significance tests: the Bonferroni method. BMJ 310:170.

Castilho, A., F. M. Dalanezi, F. F. Franchi, C. A. Price, J. Ferreira, E. Trevisol, and J. Buratini. 2019. Expression of fibroblast growth factor 22 (FGF22) and its receptor, FGFR1B, during development and regression of bovine corpus luteum. Theriogenology 125:1–5.

Chen, L., M. Wu, S. Zhang, W. Tan, M. Guan, L. Feng, C. Chen, J. Tao, L. Chen, and L. Qu. 2019. Estrogen-related receptor γ regulates hepatic triglyceride metabolism through phospholipase A2 G12B. FASEB J. 33:7942–7952.

Choi, J., W. Li, B. Schindell, L. Ni, S. Liu, X. Zhao, J. Gong, M. Nyachoti, and C. Yang. 2020. Molecular cloning, tissue distribution and the expression of cystine/glutamate exchanger (xCT, SLC7A11) in different tissues during development in broiler chickens. Anim. Nutr. 6:107–114.

Dai, W., Q. Wang, F. Zhao, J. Liu, and H. Liu. 2018. Understanding the regulatory mechanisms of milk production using integrative transcriptomic and proteomic analyses: improving inefficient utilization of crop by-products as forage in dairy industry. BMC Genom. 19:403.

Debusca, A., R. Tahergorabi, S. K. Beamer, S. Partington, and J. Jaczynski. 2013. Interactions of dietary fibre and omega-3-rich oil with protein in surimi gels developed with salt substitute. Food Chem. 141:201–208.

Galperin, E., S. Benjamin, D. Rapaport, R. Rotem-Yehudar, S. Tolchinsky, and M. Horowitz. 2002. EHD3: a protein that resides in recycling tubular and vesicular membrane structures and interacts with EHD1. Traffic 3:575–589.

Govindaraj, V., and A. J. Rao. 2015. Comparative proteomic analysis of primordial follicles from ovaries of immature and aged rats. Syst. Biol. Reprod. Med. 61:367–375.

Goyache, F., I. Fernández, A. S. R. Tapsoba, A. Traoré, N. A. Menéndez-Arias, and I. Álvarez. 2021. Functional characterization of copy number variations regions in Djallonké sheep. J. Anim. Breed. Genet. 138:600–612.

Guenter, J., and R. Lenartowski. 2016. Molecular characteristic and physiological role of DOPA-decarboxylase. Postepy. Hig. Med. Dosw. (Online) 70:1424–1440.

Hofmann, H. H., K. Heusler, K. Roth, M. J. Pröll-Cornelissen, C. Große-Brinkhaus, and K. Schellander. 2022. Oregano essential oil showed limited effects on pigs' carcass quality and haematology whereas a transcriptome analysis revealed significant modulations in the jejunum and the ileum. J. Anim. Physiol. Anim. Nutr. (Berl). 106:1017–1035.

Kulus, J., M. Kulus, W. Kranc, K. Jopek, M. Zdun, M. Józkowiak, J. M. Jaśkowski, H. Piotrowska-Kempisty, D. Bukowska, P. Antosik, P. Mozdziak, and B. Kempisty. 2021. Transcriptomic profile of new gene markers encoding proteins responsible for structure of porcine ovarian granulosa cells. Exp. Biol. Med. (Basel) 10:1214.

Li, X., Y. Lu, X. Liu, X. Xie, K. Wang, and D. Yu. 2019. Identification of chicken FSHR gene promoter and the correlations between polymorphisms and egg production in Chinese native hens. Reprod. Domest. Anim. 54:702–711.

Li, X., C. Nie, Z. Zhang, Q. Wang, P. Shao, Q. Zhao, Y. Chen, D. Wang, Y. Li, W. Jiao, L. Li, S. Qin, L. He, Y. Jia, Z. Ning, and L. Qu. 2018. Evaluation of genetic resistance to Salmonella Pullorum in three chicken lines. Poultr. Sci. 97:764–769.

Liu, J., S. Liang, X. Liu, J. A. Brown, K. E. Newman, M. Sunkara, A. J. Morris, S. Bhatnagar, X. Li, A. Pujol, and G. A. Graf. 2012. The absence of ABCD2 sensitizes mice to disruptions in lipid metabolism by dietary erucic acid[S]. J. Lipid. Res. 53:1071–1079.

Liu, S., Y. Hong, K. Cui, J. Guan, L. Han, W. Chen, Z. Xu, K. Gong, Y. Ou, C. Zeng, S. Li, D. Zhang, and D. Hu. 2018. Four-generation pedigree of monozygotic female twins reveals genetic factors in twinning process by whole-genome sequencing. Twin Res. Hum. Genet. 21:361–368.

Lu, R., and D. G. Drubin. 2017. Selection and stabilization of endocytic sites by Ede1, a yeast functional homologue of human Eps15. Mol. Biol. Cell 28:567–575.

Macarthur, C. A., and G. M. Shackleford. 1997. Npm3: a novel, widely expressed gene encoding a protein related to the molecular chaperones Nucleoplasmin and Nucleophosmin. Genomics 42:137–140.

McPhail, J. A., and J. E. Burke. 2022. Molecular mechanisms of PI4K regulation and their involvement in viral replication. Traffic 1−15. https://doi.org/10.1111/tra.12841.

Medina, M. W., F. Gao, D. Naidoo, L. L. Rudel, R. E. Temel, A. L. McDaniel, S. M. Marshall, and R. M. Krauss. 2011. Coordinately regulated alternative splicing of genes involved in cholesterol biosynthesis and uptake. PLoS One 6:e19420.

Misra, G., S. Badoni, C. J. Domingo, R. Cuevas, C. Llorente, E. Mbanjo, and N. Sreenivasulu. 2018. Deciphering the genetic architecture of cooked rice texture. Front Plant. Sci. 9:1405.

Najar, M. A., M. Arefian, D. Sidransky, H. Gowda, T. S. K. Prasad, P. K. Modi, and A. Chatterjee. 2022. Tyrosine phosphorylation profiling revealed the signaling network characteristics of CAMKK2 in gastric adenocarcinoma. Front. Genet. 13:854764.

Ødegård, J., T. H. E. Meuwissen, B. Heringstad, and P. Madsen. 2010. A simple algorithm to estimate genetic variance in an animal threshold model using Bayesian inference. Genet. Sel. Evol. 42:29.

Papatsirou, M., P. G. Adamopoulos, P. I. Artemaki, V. P. Georganti, A. Scorilas, D. Vassilacopoulou, and C. K. Kontos. 2021. Next-generation sequencing reveals alternative L-DOPA decarboxylase (DDC) splice variants bearing novel exons, in human hepatocellular and lung cancer cells. Gene 768:145262.

Pena, R. N., D. Gallardo, M. D. Guàrdia, J. Reixach, J. Arnau, and M. Amills. 2013. Appearance, flavor, and texture attributes of pig dry-cured hams have a complex polygenic genomic architecture1. J. Anim. Sci. 91:1051–1058.

Perea, C., J. F. De La Hoz, D. F. Cruz, J. D. Lobaton, P. Izquierdo, J. C. Quintero, B. Raatz, and J. Duitama. 2016. Bioinformatic analysis of genotype by sequencing (GBS) data with NGSEP. BMC Genom. 17(Suppl 5):498.

Pillai, R. A., M. O. Islam, P. Selvam, N. Sharma, A. Chu, O. C. Watkins, K. M. Godfrey, R. M. Lewis, and S. Y. Chan. 2021. Placental inositol reduced in gestational diabetes as glucose alters inositol transporters and IMPA1 enzyme expression. J. Clin. Endocrinol. Metab. 106:e875–e890.

Purcell, S., B. Neale, K. Todd-Brown, L. Thomas, M. A. R. Ferreira, D. Bender, J. Maller, P. Sklar, P. I. W. de Bakker, M. J. Daly, and P. C. Sham. 2007. PLINK: a tool set for whole-genome association and population-based linkage analyses. Am. J. Hum. Genet. 81:559–575.

Rozempolska-Rucinska, I., G. Zieba, and M. Lukaszewicz. 2013. Heritability of individual egg hatching success versus hen hatchability in layers. Poultr. Sci. 92:321–324.

Runhua, M., J. Qiang, S. Yunqing, D. Wenjun, and W. Chunsheng. 2019. FSTL3 induces lipid accumulation and inflammatory response in macrophages and associates with atherosclerosis. J. Cardiovasc. Pharmacol. 74:566–573.

Sanoudou, D., A. Duka, K. Drosatos, K. C. Hayes, and V. I. Zannis. 2010. Role of Esrrg in the fibrate-mediated regulation of lipid metabolism genes in human ApoA-I transgenic mice. Pharmacogenomics J. 10:165–179.

Sesmat, A., and J. F. Meullenet. 2001. Prediction of rice sensory texture attributes from a single compression test, multivariate regression, and a stepwise model optimization method. J. Food. Sci. 66:124–131.

Shen, M., L. Qu, M. Ma, T. Dou, J. Lu, J. Guo, Y. Hu, G. Yi, J. Yuan, C. Sun, K. Wang, and N. Yang. 2016. Genome-wide association studies for comb traits in chickens. PLoS One 11:e159081.

Silva, É. F., M. S. Lopes, P. S. Lopes, and E. Gasparino. 2019. A genome-wide association study for feed efficiency-related traits in a crossbred pig population. Animal 13:2447–2456.

Sobajima, T., S. Yoshimura, T. Maeda, H. Miyata, E. Miyoshi, and A. Harada. 2018. The Rab11-binding protein RELCH/KIAA1468

controls intracellular cholesterol distribution. J. Cell Biol. 217:1777–1796.

Song, N. J., S. Kim, B. H. Jang, S. H. Chang, U. J. Yun, K. M. Park, H. Waki, D. Y. Li, P. Tontonoz, and K. W. Park. 2016. Small molecule-induced complement factor D (Adipsin) promotes lipid accumulation and adipocyte differentiation. PLoS One 11: e162228.

Sun, S., S. Liu, J. Luo, Z. Chen, C. Li, J. J. Loor, and Y. Cao. 2019. Repeated pregnant mare serum gonadotropin-mediated oestrous synchronization alters gene expression in the ovaries and reduces reproductive performance in dairy goats. Reprod. Domest. Anim. 54:873–881.

Sun, Y., R. Liu, X. Lu, Y. Hu, G. Zhao, M. Zheng, J. Chen, H. Wang, and J. Wen. 2013. Associations of polymorphisms in four candidate genes with carcass and/or meat-quality traits in two meat-type chicken lines. Anim. Biotechnol. 24:53–65.

Sun, Y., Q. Wang, H. Jin, Z. Li, and L. Sheng. 2021. Impact of ozone-induced oxidation on the textural, moisture, micro-rheology and structural properties of egg yolk gels. Food Chem. 361:130075.

Tian, M., J. Chen, J. Li, H. Pan, W. Lei, and X. Shu. 2022. Damaging novel mutations in PIGN cause developmental epileptic-dyskinetic encephalopathy: a case report. BMC Pediatr. 22:222.

Vitorino, M., A. C. Silva, J. M. Inácio, J. S. Ramalho, M. Gur, A. Fainsod, H. Steinbeisser, and J. A. Belo. 2015. Xenopus Pkdcc1 and Pkdcc2 are two new tyrosine kinases involved in the regulation of JNK dependent Wnt/PCP signaling pathway. PLoS One 10: e135504.

Wang, Y., C. Liu, and L. Hu. 2019. Cholesterol regulates cell proliferation and apoptosis of colorectal cancer by modulating miR-33a-PIM3 pathway. Biochem. Biophys. Res. Commun. 511:685–692.

Wen, Y., H. Zhang, Y. Ni, B. Huang, J. Zhang, J. Feng, S. Wang, J. M. Dunwell, Y. Zhang, and R. Wu. 2018. Methodological implementation of mixed linear models in multi-locus genome-wide association studies. Brief. Bioinform. 19:700–712.

Weng, K., Y. Li, W. Huo, Y. Zhang, Z. Cao, Y. Zhang, Q. Xu, and G. Chen. 2022. Comparative phosphoproteomic provides insights into meat quality differences between slow- and fast-growing broilers. Food Chem. 373:131408.

William, A., and J. B. David. 2009. Population structure and cryptic relatedness in genetic association studies. Stat. Sci. 24:451–471.

Winham, D. M., M. E. Tisue, S. M. Palmer, K. A. Cichy, and M. C. Shelley. 2019. Dry bean preferences and attitudes among midwest hispanic and non-hispanic white women. Nutrients 11:178.

Xiao, N., Y. Zhao, Y. Yao, N. Wu, M. Xu, H. Du, and Y. Tu. 2020. Biological activities of egg yolk lipids: a review. J. Agr. Food Chem. 68:1948–1957.

Xiao, Y., H. Liu, L. Wu, M. Warburton, and J. Yan. 2017. Genome-wide association studies in maize: praise and stargaze. Mol. Plant. 10:359–374.

Xu, H., L. Ju, Y. Xiong, M. Yu, F. Zhou, K. Qian, G. Wang, Y. Xiao, and X. Wang. 2021. E3 ubiquitin ligase RNF126 affects bladder cancer progression through regulation of PTEN stability. Cell Death Dis. 12:239.

Yang, Y., Y. Zhao, M. Xu, Y. Yao, N. Wu, H. Du, and Y. Tu. 2020. Effects of strong alkali treatment on the physicochemical properties, microstructure, protein structures, and intermolecular forces in egg yolks, plasma, and granules. Food Chem. 311:125998.

Yu, J., J. Chia, C. A. Canning, C. M. Jones, F. A. Bard, and D. M. Virshup. 2014. WLS retrograde transport to the endoplasmic reticulum during Wnt secretion. Dev. Cell 29:277–291.

Zhang, B., Y. Jia, Y. Yuan, X. Yu, Q. Xu, Y. Shen, and Y. Shen. 2004. No association between polymorphisms in the DDC gene and paranoid schizophrenia in a northern Chinese population. Psychiatr. Genet. 14:161–163.

Zhang, H., L. Shen, Y. Li, Z. Xu, X. Zhang, J. Yu, Z. Cao, and P. Luan. 2019. Genome-wide association study for plasma very low-density lipoprotein concentration in chicken. J. Anim. Breed. Genet. 136:351–361.

Zhang, R., J. Deng, X. Li, W. Shang, and Z. Ning. 2022. Research Note: Comparison of the texture, structure, and composition of eggs from local Chinese chickens and a highly selected line of egg-type chickens and analysis of the effects of lipids on texture. Poultr. Sci. 101:101934.

Zhang, Z., Z. Zhang, F. O. Oyelami, H. Sun, Z. Xu, P. Ma, Q. Wang, and Y. Pan. 2021. Identification of genes related to intramuscular fat independent of backfat thickness in Duroc pigs using single-step genome-wide association. Anim. Genet. 52:108–113.

Zhao, Y., F. Feng, Y. Yang, C. Xiong, M. Xu, and Y. Tu. 2021. Gelation behavior of egg yolk under physical and chemical induction: a review. Food. Chem. 355:129569.

Zhou, X., and M. Stephens. 2012. Genome-wide efficient mixed-model analysis for association studies. Nat. Genet. 44:821–824.

Zhu, L., A. Yang, Y. Mu, N. Zhang, L. Sun, S. A. Rajput, and D. Qi. 2019. Effects of dietary cottonseed oil and cottonseed meal supplementation on the structure, nutritional composition of egg yolk and gossypol residue in eggs. Poultr. Sci. 98:381–392.